ELSEVIER

Journal of Nuclear Materials 220–222 (1995) 269–273

journal of nuclear materials

Surface erosion issues and analysis for dissipative divertors ☆

J.N. Brooks [a], D.N. Ruzic [b], D.B. Hayden [b], R.B. Turkot Jr. [b]

[a] *Argonne National Laboratory, 9700 South Cass Avenue, Argonne, Illinois 60439, USA*
[b] *University of Illinois, 103 South Goodwin Avenue, Urbana, Illinois 61801, USA*

Abstract

Erosion/redeposition is examined for the sidewalls of a dissipative divertor using coupled impurity transport, charge exchange, and sputtering codes, applied to plasma solutions for the ITER design. A key issue for this regime is possible runaway self-sputtering, due to the effect of a low boundary density and nearly parallel field geometry on redeposition parameters. Net erosion rates, assuming finite self-sputtering, vary with wall location, boundary conditions, and plasma solution, and are roughly of the following order. 200–2000 Å/s for beryllium, 10–100 Å/s for vanadium, and 0.3–3 Å/s for tungsten.

1. Introduction

There is currently much interest in divertor plasma regimes that dissipate heat primarily by radiation and charge exchange and not by highly peaked convective heat flow to the boundary surfaces. It is not clear, however, if these regimes offer advantages in terms of surface erosion and, in fact, some of the erosion problems appear to be worse. We have started to study this subject by analyzing sputtering erosion for a dissipative divertor for the ITER design, using plasma parameters found by Petravic et al. [1] (PPPL solution). We have also made preliminary use of the plasma solutions of Schmitz et al. [2] (UCLA solution) and Knoll et al. [3] (INEL solution). The materials considered are beryllium, vanadium, tungsten, and lithium (liquid metal).

The plasma regimes used here and many under study worldwide are highly speculative and involve considerable physics uncertainties, particularly regarding boundary conditions. The goal of the present analysis is to identify broad trends and define research needs. The analysis should clearly not be taken as providing reliable design-specific erosion predictions. The latter will require an extensive, coordinated effort, together with experimental verification.

Our analysis uses coupled computer code calculations to examine: (1) the microstructure of sputtered particle transport at and near a dissipative divertor sidewall point, using the WBC code [4,5] (2) the charge exchange flux to the divertor sidewalls and plate given the ion flux from a plasma solution-DEGAS code [6], and (3) impurity transport and erosion over the entire sidewall-REDEP code [5,7]. Also, the Vectorized Fractal TRIM (VFTRIM) code [8] has been used to compute selected sputtering coefficients where needed, including a complete set for beryllium.

2. Model

We model the dissipative divertor conceptually, Fig. 1, as a toroidally symmetric plasma channel formed between two sidewalls and a plate. In theory, hot scrape-off layer plasma flows into the channel from the top and is cooled/extinguished at the plate due to intense neutral gas recycling or by impurity induced radiation. The top portion of the sidewalls in this model can correspond to various baffle or "guard plates" of detailed designs e.g., Ref. [9]. A key issue for the dissipative divertor is whether close-fitting sidewalls receiving a significant ion flux are necessary. This

☆ Work supported by the United States Department of Energy, Office of Fusion Energy.

SSDI 0022-3115(94)00426-9

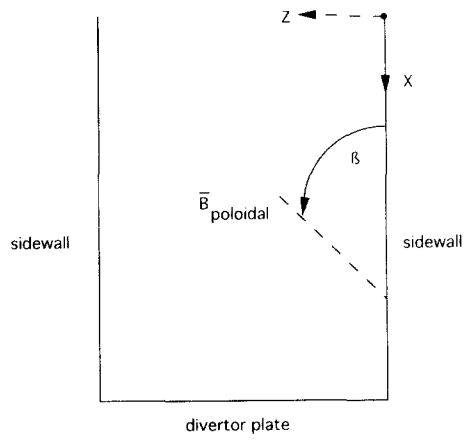

Fig. 1. Model geometry.

appears to be the case, for the plasma regimes examined [1–3], in order to insure adequate neutral baffling. (The ion boundary flux may be much lower for regimes involving injected impurities e.g., Ref. [10]. Charge exchange fluxes remain high, however. The feasibility of this or any approach to achieving dissipative conditions is highly uncertain.)

An engineering design will likely have both poloidally and toroidally discontinuous walls (e.g., a tube structure) and a complex magnetic field angle-to-surface geometry. Although field-parallel sidewalls are commonly assumed in various plasma simulations it is easily shown that this is virtually impossible in practice. To roughly model an actual situation we assume continuous walls, but with specified non-zero angles α, β for the total field and poloidal field, respectively. Except where otherwise indicated, we use $\beta = 3°$, $\alpha = 1°$. This contrasts with a "conventional" divertor where most erosion occurs at the divertor *plate* and where typically $\beta = 15$–$30°$ and $\alpha = 3°$.

In the present plasma solutions the ion flow to the sidewall vicinity is assumed to occur by diffusion. At the wall, however, convective flow along intersecting field lines may dominate. The formation of a plasma sheath at the sidewall appears likely. This sheath is modeled as having the dual spatial structure (magnetic and Debye regions) of Ref. [4] and with a locally-varying potential of $e\phi(x) = 3kT_e(X, 0)$, for electron temperature $T_e(X, Z)$.

The plasma at the dissipative divertor sidewall-boundary differs from the conventional high recycling plate-boundary plasma in at least two respects: (1) the plasma density at the boundary is much lower ($\sim 10\times$) but may have a high local gradient, and (2) as discussed, the magnetic field angle is uncertain, but is likely to be more tangential. This may result in significant differences in the transport of sputtered impurities. To examine this, and to provide necessary redeposition parameter input to the REDEP large-scale erosion/redeposition code, we used the WBC Monte Carlo code for detailed examination of sputtered particle transport at/near a typical sidewall point.

For the WBC simulations, particles are launched with a velocity distribution corresponding to a mix of D–T and self-sputtering. The code then computes the charge-changing and velocity-changing collisions with the plasma, and the sub-gyro orbit motion due to the magnetic field and sheath electric field. Bohm type diffusion is included. Each simulation uses 1000 particles. A particle history terminates upon being redeposited on the surface or "lost" to the plasma ($Z \geq 0.03$ m).

Following the WBC calculations, REDEP erosion/redeposition code was used to compute overall sidewall erosion for the PPPL plasma solution. The latter uses the PLANET [1] fluid code to provide the 2-D profiles of density temperature, and ion flux. In addition to the PLANET code supplied D–T ion flux we have as-

Table 1
Summary of impurity transport parameters, from WBC analysis of a dissipative divertor sidewall point, $T_e = 30$ eV, $N_{e_0} = 10^{19}$ m^{-3}, $N_{e_1} = 10^{20}$ m^{-3}, $\alpha = 1°$

Parameter [a]		Lithium	Beryllium	Vanadium	Tungsten
Neutral ionization distance					
(perp. to surface)	$\bar{Z}_0$ [mm]	5.0	5.2	0.7	1.6
Charge state	$\bar{K}$	1.1	1.8	2.0	3.2
	K_{SD}	0.3	0.4	1.1	2.2
Ion transit time	$\bar{\tau}$ [μs]	18	13	6	9
Elevation angle	$\bar{\theta}$ [deg.]	58	61	25	31
(from normal)	θ_{SD} [deg.]	7	8	14	16
Energy	$\bar{U}$ [eV]	136	233	247	475
	U_{SD} [eV]	61	80	240	481
Self-sputtering coefficient	$\bar{Y}_{Z,Z}$	1.3	1.4	0.55	0.60

[a] Bar denotes average, SD denotes standard deviation, of redeposited particles.

sumed a He^{2+} flux and oxygen ion flux of 10% and 0.1% respectively of the D–T ion flux. The DEGAS Monte Carlo code was used to compute the D–T charge exchange (CX) flux to the wall, given input plasma parameters from PLANET. The DEGAS calculation includes the effects of volume recombination and wall recycling on the CX flux. Both beryllium and tungsten walls were investigated, with energy and angle resolved rough-surface wall reflection coefficients for hydrogen taken from VFTRIM. Sputtering coefficients in WBC and REDEP are computed by averaging over the relevant incident ion and neutral energy and angular distributions. For D^+, T^+, He^{2+} on Be, and all self-sputtering coefficients, calculations from VFTRIM were used. A fractal dimension of 2.08 was used to simulate typical surface roughness. For D^+, T^+, He^{2+}, on vanadium and tungsten, a variety of models as described in Refs. [5,7] were employed.

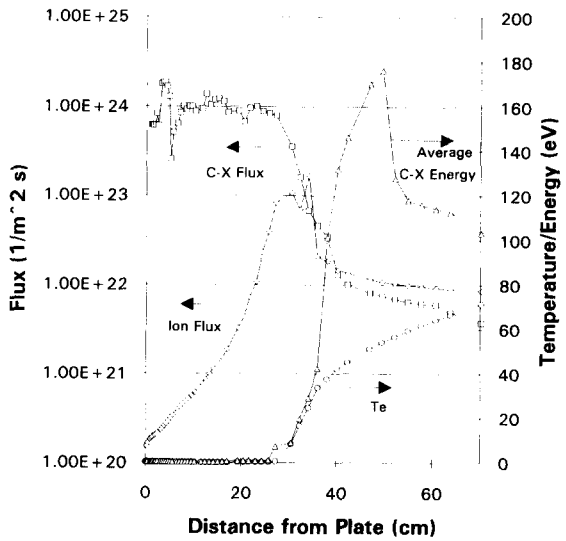

Fig. 2. Ion flux, electron temperature, and charge exchange parameters along the sidewalls for the PPPL [1] solution.

3. Results

3.1. WBC analysis of impurity transport at a side wall point

Table 1 summarizes the impurity transport results for the typical case of plasma temperature $T_e = 30$ eV, and density $N_{e0} = 1 \times 10^{19}$ m^{-3} at the sheath. The density profile at the boundary is important to the erosion process, but is not well specified in the various plasma solutions. For this calculation the density is assumed to be constant from just outside the sheath to 3 mm away, and then to rise linearly in the next 1 cm to a value of $N_{e1} = 10^{20}$ m^{-3}. (Other density profiles were also surveyed.) As expected, the low density at the wall is of key importance to the transport. Compared to results [4,5] for a high recycling divertor having an order of magnitude higher density at the sheath, sputtered V^0 and W^0 atoms are ionized primarily outside the sheath. This results in a longer redeposition time (due also to the nearly parallel field angle), and higher plasma-impurity energy equilibration, attained charge states, and sheath acceleration. Beryllium is ionized outside of the sheath for "conventional" conditions also, but is found to also acquire a somewhat higher charge state and redeposited energy. Also, due in part to the weaker Debye region electric field, redeposited ions impact at more oblique incidence.

At this temperature the self-sputtering coefficients are less than unity for vanadium and tungsten. They exceed unity for lithium and beryllium. The high self-sputtering coefficient for the low-Z materials is due to their oblique incidence, a theoretical trend discussed in detail in Refs. [11,12]. (Some recent data [13], however, shows substantial deviations from theory and points to the need for low-energy, oblique incidence, self-sputtering data.)

3.2. REDEP analysis - PPPL plasma solution

Fig. 2 shows the PPPL plasma and DEGAS-computed CX parameters along the sidewall (for the Be wall case). The CX energy is a function of ion temperature (not shown but fairly similar to T_e) both at the boundary and in the bulk of the divertor plasma. Although only the average CX energy is shown, the REDEP calculations use the DEGAS computed CX energy spectrum for sputtering calculations. The peak in ion flux near the sidewall bottom is a key feature of this plasma solution, resulting from the transition between the hot plasma and extinguished plasma. It is not clear how fundamental such a peak is – it is not present in the UCLA solution, but that is for a considerably lower input power.

Using the model described, the REDEP analysis predicts a self-sputtering runaway situation for all four materials examined. This results from a combination of high self-sputtering coefficients and the obtained redeposition profile. We conclude that this is a significant issue for the PPPL plasma solution. To account for the numerous model uncertainties, however, and for further scoping purposes, we continued the REDEP analysis with all self-sputtering coefficients bounded by: $Y_{Z-Z} \leq 0.5$. The cases to be described use this constraint with all other parameters unchanged.

Fig. 3 shows the gross erosion rate (sputtering only) and Fig. 4 the net erosion rate (sputtering minus redeposition) for Be, V, and W. The gross erosion profile

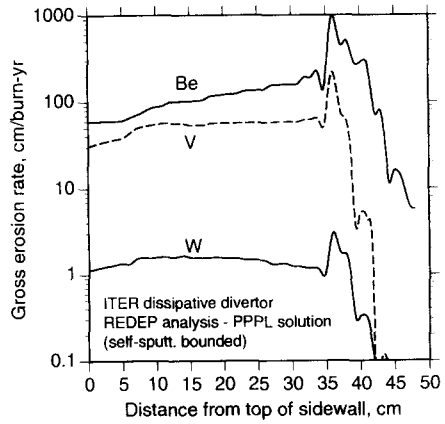

Fig. 3. Gross erosion rate for the dissipative divertor sidewall.

for lithium (not shown) is similar to the beryllium case shown. As discussed, these rates are computed for uniform continuous walls but represent a rough toroidal average for toroidally irregular walls. The gross erosion profiles are characterized by: (1) a wide region 0 ~ 35 cm from the top having fairly uniform erosion, (2) a sharp peak due to the flux peak at the plasma "transition" zone, and (3) a diminishing rate towards the plate where the plasma becomes extinguished. The big difference in gross erosion rates for the different materials is primarily due to differences in the D–T sputtering coefficients.

For all materials and particularly beryllium the local redeposition fraction over much of the surface is lower than for a conventional divertor, e.g., see Refs. [5,7], due to the much shallower poloidal angle (i.e., 3° versus ~ 15°) and lower boundary electron density. For beryllium the net erosion rate is within about a factor of 2 of the gross rate, except near the bottom of the wall where substantial *growth* occurs. This growth is

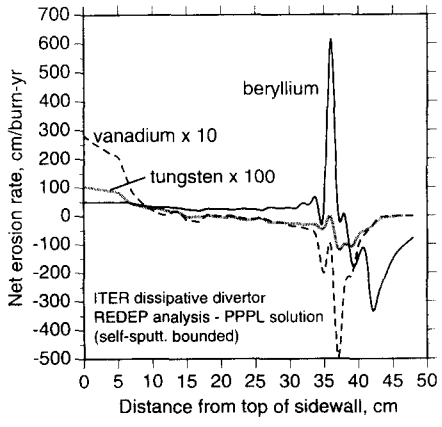

Fig. 4. Net erosion rate for the dissipative divertor sidewall.

Table 2
REDEP dissipative divertor sidewall erosion analysis – peak net erosion rate as a function of model parameter variations

Parameter		Peak net erosion rate, cm/burn yr		
		Beryllium	Vanadium	Tungsten
"Reference values" [a]		689	28	1.1
Poloidal angle $\beta = 0$		835	89	1.4
	6°	599	27	1.0
Sheath potential $\frac{e\phi}{kT_e} = 0$		175	7	0.10
	6	858	43	2.7

[a] $\beta = 3°$, $\frac{e\phi}{kT_e} = 3$, self-sputtering coefficients ≤ 0.5 (see text).

due to a transfer of sputtered material from top to bottom. Vanadium exhibits a much higher peak redeposition fraction than beryllium, due to shorter ionization distances (e.g., as shown in Table 1). This results from lower sputtered velocities and a higher rate coefficient for electron impact ionization. Tungsten, likewise, is redeposited at a higher rate than beryllium but less so than for a high recycling divertor. Both Be and Li erosion rates, while high in terms of a surface issue, represent only a small perturbation of the boundary plasma with impurity ions. For all materials little or no contamination of the plasma away from the wall is predicted, due to confinement of sputtered atoms to the near surface (~ 0–3 cm) region, and redeposition at *some* point on the wall.

3.3. Other cases

The effect of several parameter variations on the erosion for the PPPL solution was examined. (Due to present model limitations these calculations are not self-consistent, e.g., particle flux would likely change with different poloidal angles, but this was not modeled.) The peak net erosion rates are shown in Table 2. A value of $\beta = 0$ results in no redeposition whatever (neglecting a diffusional effect), and hence no self-sputtering, while a value of $\beta = 6°$ represents a less oblique geometry than the reference value. As shown, this affects vanadium more than the other materials. A sheath potential variation affects all materials significantly, primarily by increasing the D, T, and He impingement energy, and is particularly critical for tungsten.

A brief, preliminary, analysis was made of sidewall erosion for the UCLA [2] and INEL [3] solutions. These solutions also involve most input power to the divertor being dissipated by hydrogen recombination radiation, charge exchange, and in the case of Ref. [3], by beryllium impurity radiation as well. Numerous differences among these solutions exist, in particular, the assumed divertor input power and midplane density for

solutions of Refs. [1–3] are: 220 MW, 133 MW, 200 MW, and 1.4×10^{20} m^{-3}, 1.0×10^{20} m^{-3}, and 5×10^{19} m^{-3} respectively. The peak temperature at the sidewall (top) for solutions [2,3] is $T_e \approx 15$ eV. (None of these solutions are consistent with impurities generated from sputtering and radiation, if any, that may occur from them.) The present analysis computed erosion at and near the top of the sidewall only, for beryllium and tungsten. The net erosion rate for beryllium, at the top, is ~50 and ~150 cm/burn yr, for solutions of Ref. [2] and Ref. [3], respectively. For tungsten, the net rate is ~0.1 cm/burn yr which results only from sputtering by the trace oxygen content, and by self-sputtering.

4. Conclusions

The present analysis shows the following trends:

(1) Runaway self-sputtering at the dissipative divertor sidewall is a potential problem for all materials examined, for the relatively high edge temperature plasma solution studied. Self-sputtering may set an upper limit on the acceptable boundary plasma temperature. The temperature limit may be more restrictive (lower edge T_e allowed) for the low-Z materials due to the highly oblique incidence of the redeposited ions.

(2) Local redeposition fractions for the sidewall are lower than for a conventional divertor plate due to a lower boundary electron density and more tangential poloidal field geometry.

(3) Erosion rates for beryllium appear very high. A 5 mm Be coating, for example, could be eroded in as few as 25×1000 s burn pulses, even assuming a no-runaway sputtering situation. Extrapolation of beryllium use to commercial fusion reactor conditions appears very difficult. Preliminary results for Be are potentially better, but still discouraging, for plasma solutions involving less input power or lower mid-plane density.

(4) Vanadium erosion is an order of magnitude lower than beryllium, all other things being equal. Tungsten erosion is potentially 2–4 orders of magnitude lower than beryllium.

(5) Sputtered atoms of vanadium and tungsten appear likely to be confined to the near-boundary region and so would not affect the bulk of the divertor plasma. This is true of lithium and beryllium under most, but not all of the conditions surveyed.

Future work is planned on a full analysis of plasma solutions [2,3], including plate erosion, and on additional dissipative plasma regimes that may be identified. Critical modeling issues include boundary conditions in general, effect of toroidal and poloidal discontinuities, sheath effects, pre-sheath and/or other electric fields, and potential sputtering due to injected radiation enhancing impurities. If carbon is included as a wall material, critical modeling issues would include the effect of the different boundary parameters on chemically sputtered particle transport.

References

[1] M. Petravic, G. Bateman, and D. Post, Proc. 4th Int. Workshop on Plasma Edge Theory in Fusion Devices, Varenna, 1993; to be published.
[2] L. Schmitz, B. Merriman, personal communication (1994).
[3] D.A. Knoll, R.B. Campbell, and P.R. McHugh, Contrib. Plasma Physics, to be published.
[4] J.N. Brooks, Phys. Fluids 8 (1990).
[5] J.N. Brooks, in: *Atomic and Plasma-Material Interaction Processes in Controlled Thermonuclear Fusion*, R.K. Janev and H.W. Drawin, eds. (Elsevier, Amsterdam, 1993) pp. 403–427.
[6] D.B. Heifetz, D. Post, M. Petravic, J. Weisheit and G. Bateman, J. Comp. Phys. 46 (1982) 309.
[7] J.N. Brooks, Nucl. Technol. Fusion 4 (1983) 33.
[8] D.N. Ruzic, Nucl. Instr. and Meth. B 47 (1990) 118.
[9] US Design Support Study for the ITER Divertor, ITER/US/93/IV-PF-3 (1993).
[10] G. Janeschitz, J. these Proceedings (PSI-11), J. Nucl. Mater. 220–222 (1995) 73.
[11] J. Roth, in: *Atomic and Plasma Material Interaction Processes in Controlled Thermonuclear Fusion*, R.K. Janev and H.W. Drawin, eds. (Elsevier, Amsterdam, 1993) pp. 381–401.
[12] W. Eckstein, J. Bohdansky, J. Roth, Nucl. Fusion Suppl. 1 (1991) 51.
[13] E. Hechtl, J. Roth, W. Eckstein, and C. Wu, these Proceedings (PSI-11), J. Nucl. Mater. 220–222 (1995) 883.